Appl. Phys. B 42, 21–29 (1987)

Applied Physics B Photophysics and Laser Chemistry

Investigation of the Dynamic Recording Process of Thick Refractive Index Gratings in Photorefractive Crystals by the Microphotometric Method

R. A. Rupp

Fachbereich Physik, Universität, D-4500 Osnabrück, Fed. Rep. Germany

Received 6 June 1986/Accepted 20 September 1980

Abstract. Diffraction-efficiency measurements are compared with the microphotometric determination of the intensity pattern at the exit face of a $LiNbO_3$-sample during the holographic recording process. The special advantage of the microphotometric method is the possibility to determine phase shifts of the refractive index grating and of the light intensity pattern simultaneously and independently. Both quantities are very important for an understanding of dynamical effects during the holographic writing process. Furthermore, direct experimental evidence for the change of the modulation degree, i.e. the change of the contrast of the light pattern writing the grating, has been found. This change is caused by a Moiré-like effect which is closely related to the energy transfer between writing beams.

PACS: 42.30, 42.40, 42.70

In recording experiments of elementary volume phase holograms utilizing electrooptic crystals the refractive-index grating and the fringe pattern of the interfering beams shift as a function of time. The reason is the feedback of the just written hologram on the writing light intensity pattern [1]. This so-called self-diffraction is usually investigated by beam-coupling experiments [2]. However, it is not possible to investigate higher-order Fourier components by beam coupling experiments, and diffraction efficiency measurements [3] are not sensitive to phase shifts. Up to now there is also a lack of a reliable method to determine the phase shifts of the grating and of the interference pattern independently. These quantities are the key parameters for a deeper understanding of the dynamics of the writing process and the underlying electronic transport mechanism [4].

For this purpose we propose imaging of the refractive-index gratings with a transmission microscope. This has several advantages compared to the methods mentioned before: Firstly, even white-light illumination provides a good image contrast [5]. Secondly, transmission microscopy permits also a local determination of the refractive-index amplitude and phase shift, whereas diffraction efficiency and beam coupling furnish only data averaged over the whole sample. Thirdly, also the time dependence of the phase shift of the illuminating interference pattern can be obtained independently. In the fourth place, the experimental set-up can be designed for real-time investigations of contrast and phase during the grating build-up, simultaneously tracking not only the first but also higher Fourier components. In the fifth place, we can also analyse the depth profile of the grating.

The contrast formation process was theoretically and experimentally investigated in [6]. The physics of two limiting cases can be easily understood: The first case is imaging by the waveguiding properties of the grating. A planar grating consists of planes with constant refractive index. A layer which contains the plane with the highest refractive index is surrounded by the layers with lower refractive index. This structure acts like a planar waveguide for a nearly normally incident plane wave. Thus intensity is "concentrated"

in those layers with high refractive index and at the exit face of the thick grating a modulated intensity pattern appears. For normal incidence it can be deduced from symmetry considerations, that light intensity and refractive-index maxima coincide. The second case is imaging by Bragg diffraction. The diffracted and transmitted waves interfere at the exit plane and the resulting near-field interference pattern can be scanned photometrically. In contrast to the previous case this pattern is shifted by $\pi/2$ against the refractive index grating. The shift directions has been determined in [6]. Hence both cases permit the determination of the position of the grating and its phase shift with time during the recording process. Furthermore, the amplitudes of the periodic intensity patterns are proportional to the refractive index amplitude as long as the amplitudes remain small. Imaging by the waveguide properties has the advantage of producing a "true" image, which is easy to interpret, because the intensity modulation is not only proportional but also in phase to the refractive index modulation. On the other hand, the contrast is usually much higher for imaging by diffraction at the Bragg angle.

Our theoretical analysis proceeds from the so-called Floquet-Bloch or modal theory for the wave propagation in thick sinusoidally modulated dielectric media [6]. This approach provides more physical insight than coupled-wave theory [7]. Tamir et al. derived the dispersion equation for H-modes and show how to calculate the Floquet solutions numerically via continued fractions [8, 9]. They also gave analytical results for small modulations far from the band edge and the form of the field and phase variation of a Floquet mode. But they discussed only line-source excitation, plane-wave excitation for grating planes parallel to the boundary of a modulated half plane and the excitation of a modulated waveguide. It was Burckhardt who first applied the theory to the sinusoidally modulated slab, which is the common configuration of an unslanted transmission hologram [10]. He worked out the E- and the H-mode case in detail. Beyond that, we analysed an arbitrary periodic grating with a depth profile and include not only the fundamental, but all space harmonics of the incident wave to account also for beam coupling phenomena [11]. The experimentally determined first and second Fourier component of the intensity pattern as well as the phase of the first Fourier component show satisfactory agreement with calculations for a planar grating characterized by two Fourier coefficients and the phase shift between the first and second Fourier component of the dielectric grating.

In this paper we compare diffraction efficiency measurements with photometric measurements of the first and second Fourier component of the intensity pattern. Then we consider the calculation of the refractive index amplitude in the presence of light-induced scattering. Further we present results on the phase shift of the writing light intensity pattern, on the phase shift of the refractive-index grating, and the change of the light-intensity modulation during writing. These dynamic effects are closely related to beam-coupling phenomena. We think these possibilities indicate that microphotometry is a promising method to analyse the dynamic writing process in photorefractive crystals.

1. Experimental

The thick holographic gratings investigated were recorded with an argon-ion laser operated at the wavelength $\lambda_0 = 514.5$ nm in an usual holographic arrangement (Fig. 1). The components were mounted on a vibration isolated table and enclosed in a plexiglass cover to prevent air turbulences which cause random fluctuations of the optical path length. A major problem were drifts due to thermal expansion. Before starting the experiments the samples were heated for half an hour to approximately 300° C in order to erase former gratings. After cooling down to room temperature the *c*-axis faces of the sample were short-circuited with silver paste. Complications due to the so-called transient energy exchange [1] were avoided by the choice of exactly equal writing intensities. The transmitted far-field intensities I_0, I_{+1}, and I_{-1} were measured by three silicon detectors. The light intensity distribution at the exit face of the crystal was recorded by a silicon array detector (optical multichannel analyser 1453, EG & G Instruments) with 1024 pixels after magnification ($V = 67x$) by a microscope.

In certain time intervals the writing process was interrupted by the shutters S_+ and S_-, respectively. From the intensities I_+ and I_- during read-out the diffraction efficiencies

$$\eta_+ = \frac{I_{+1}}{I_{+1}+I_{-1}}, \quad \text{with} \quad I_{+10}=0 \quad \text{and} \quad I_{-10}\neq 0 \tag{1}$$

and

$$\eta_- = \frac{I_{-1}}{I_{+1}+I_{-1}}, \quad \text{with} \quad I_{-10}=0 \quad \text{and} \quad I_{+10}\neq 0 \tag{2}$$

were determined.

Simultaneously the image intensity was measured by the microphotometric assembly to evaluate the amplitude and the phase shift of the refractive-index grating from the contrast and phase shift of the image observed at the Bragg angle Θ_0. The data records of the

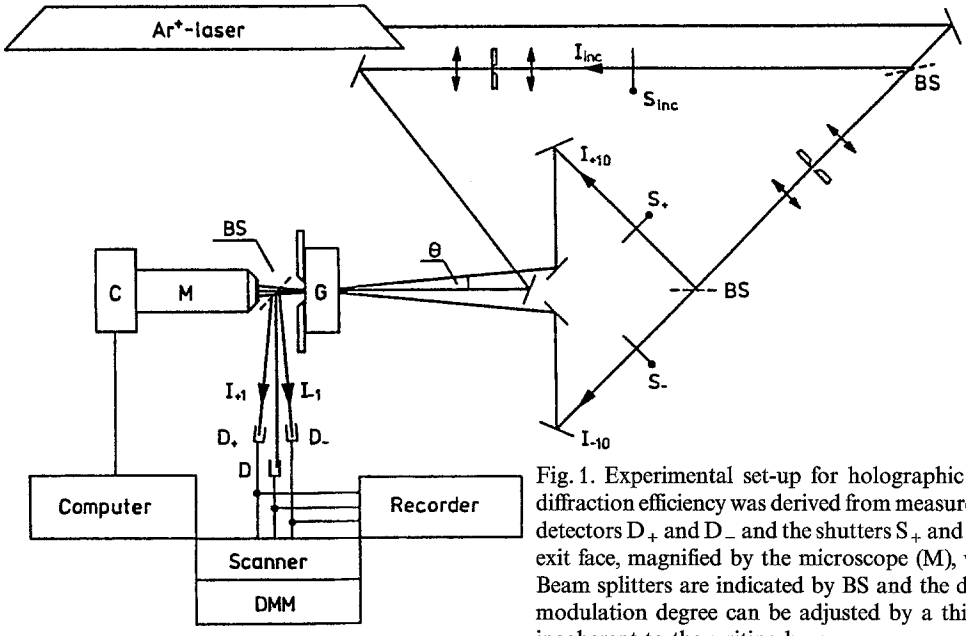

Fig. 1. Experimental set-up for holographic writing of the grating (G). The diffraction efficiency was derived from measurements with the help of the silicon detectors D_+ and D_- and the shutters S_+ and S_-, respectively. The image at the exit face, magnified by the microscope (M), was recorded by the camera (C). Beam splitters are indicated by BS and the digital multimeter by DMM. The modulation degree can be adjusted by a third beam with the intensity I_{inc}, incoherent to the writing beams

Table 1. Data [11] characterizing the investigated thick refractive index gratings

Sample	A	B
Material	$LiNbO_3:Fe$	
$c_{Fe^{2+}}$ [cm^{-3}]	6.3×10^{17}	
$c_{Fe^{3+}}$ [cm^{-3}]	6.9×10^{18}	
σ_{ph}/I_0 [$cm\,V^{-2}$]	9×10^{-14}	
E_{ph} [$kV\,cm^{-1}$]	42	
d [μm]	930	
Λ [μm]	6.02	6.12
η	0.58	0.53
Observation polarization	Ordinary	Extraordinary
q	0.19	0.57

$c_{Fe^{2+}}$ Fe^{2+} concentration
$c_{Fe^{3+}}$ Fe^{3+} concentration
σ_{ph}/I_0 specific photoconductivity
E_{ph} photovoltaic field
d thickness
Λ grating spacing
η diffraction efficiency at the end of the writing process (ordinarily polarized light)

intensity patterns were tapered with a Hamming window. After Fourier transformation the prominent intensity components at the spatial frequencies $k=vG$ ($v=0,1,2,\ldots$) of the grating can be recognized easily and separated from artifacts. The fundamental spatial frequency

$$G=\frac{4\pi}{\lambda_0}\sin\Theta_0 \tag{3}$$

is calculated from the wavelength λ_0 and the half angle Θ_0 between the writing beams. Quantities with index "0" are measured in air. The intensity components $I(vG)$ and $I(0)$ at the spatial frequencies $k=vG$ and $k=0$ were first divided by the empirically determined modulation transfer function of the measurement system. Then the contrast components defined by

$$B(vG)=\frac{I(vG)}{I(0)}, \qquad v=1,2,3,\ldots \tag{4}$$

were calculated. The phase of the intensity pattern follows directly from the Fourier transformed data record and is refered to the phase of the intensity pattern at the beginning of the writing process, which is defined to be zero.

Data characterizing the two samples which were investigated are given in Table 1. They are partially used as input data for the analysis of the measurements. The samples are identical with those described in [6].

2. Contrast and Diffraction Efficiency

Interrupting one writing beam at several stages of the writing process for a short time interval, the efficiency η of the first Bragg diffraction order and the first-order Fourier coefficient $B(G)$ of the corresponding microscopic image pattern can be determined simultaneously as outlined in the preceeding section. At first we compare the experimental data with the theoretical results of the two-beam approximation [6], which

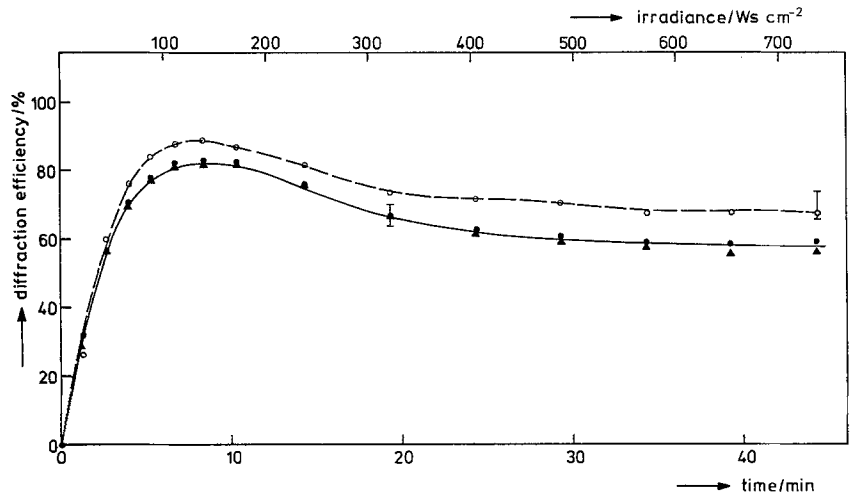

Fig. 2. Time dependent development of the diffraction efficiency η_+ and η_- (full dots and triangles) and corresponding values calculated via (5) from the contrast B(G) (open circles) for sample A

claims that the following relation holds

$$B(G)=\sin\left(\frac{2\pi\Delta nd}{\lambda_0\cos\Theta}\right)=2\sqrt{\eta(1-\eta)}\,. \tag{5}$$

Here Δn is the refractive index amplitude, d the grating thickness and Θ the Bragg angle in the material. Figure 2 shows the diffraction efficiencies η_+ (full dots) and η_- (full triangles) as a function of time or exposure, respectively. Within the scope of measurement accuracy we find the diffraction efficiency to be independent of the direction of the reading beam. Hence the writing process exhibits no asymmetric diffraction resulting, e.g., from an additional phase shifted absorption grating. This phenomenon has been discussed recently by Guibelalde [12]. On the other hand, the diffraction efficiency can be calculated from the first Fourier component of the intensity pattern via (5). The values are also shown in Fig. 2 (open circles). Considering the error margins, it may be concluded, that the efficiency values derived from the contrast $B(G)$ are systematically too large after about four minutes of writing.

The reason for this discrepancy is the following: Though the assumption of a two-beam case is usually quite adequate for the diffraction efficiency, it is not for the contrast, because the contrast turns out to be under certain circumstances much more sensitive to higher order diffraction components. In order to find an explanation for this fact we assume a diffraction far field consisting of $j=0,1,\ldots,N$ planar waves with intensities I_j and phases ϕ_j. The diffraction efficiency of the j-th order is defined by $\eta_i=I_j/\bar{I}$, where $\bar{I}=\Sigma_j I_j$ and the interference pattern at the exit face is given by

$$I(z)=\bar{I}\left\{1+\sum_{j\neq k}\sum_{k} m_{jk}\cos[(j-k)Gz+\phi_{jk}]\right\}$$

with $\phi_{jk}=\phi_j-\phi_k$ and $m_{jk}=2\sqrt{I_jI_k}/\bar{I}=2\sqrt{\eta_j\eta_k}$. Now it is easy to see, that in the case of three diffraction orders the fundamental contrast component contains contributions of the second-order diffraction

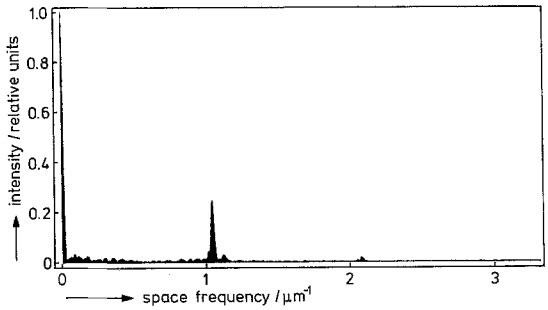

Fig. 3. Fourier transform spectrum of the image during read out at Bragg angle 10 minutes after beginning of the writing process (sample A)

$$\begin{aligned}I(z)&=\bar{I}[1+m_{01}\cos(Gz-\phi_{01})\\&\quad+m_{12}\cos(Gz-\phi_{12})+m_{02}\cos(2Gz-\phi_{02})]\\&=\bar{I}[1+m_{012}\cos(Gz-\phi_{012})+m_{02}\cos(2Gz-\phi_{02})]\end{aligned}$$

Between these quantities there are the relations $\phi_{12}=\phi_{01}-\phi_{02}$, $m_{12}=2\eta_1 m_{02}/m_{01}$, and $\eta_0\approx 1-\eta_1$ for η_2 small compared to η_1. So we must admit the possibility of an appreciable contribution to m_{012} induced by η_2 even if η_2 remains negligable compared to η_1 and η_0. This is true, as soon as η_1 is larger than η_0. But nevertheless we should also notice the component m_{02} in the light-intensity pattern. In fact this component is ascertainable shortly after the beginning of the writing process in the contrast spectrum reaching saturation approximately at the same time as the first-order contrast Fourier component (Fig. 3). The time dependence is indicated in Fig. 4 by full dots. Because η_1, m_{012}, m_{02}, and ϕ_{02} can be evaluated at each time from the measurements (Table 2), the results of Fig. 2 can be corrected for the second-order Fourier components, leading to satisfactory agreement of the diffraction efficiency measurements with the contrast measurements, as presented in Fig. 5.

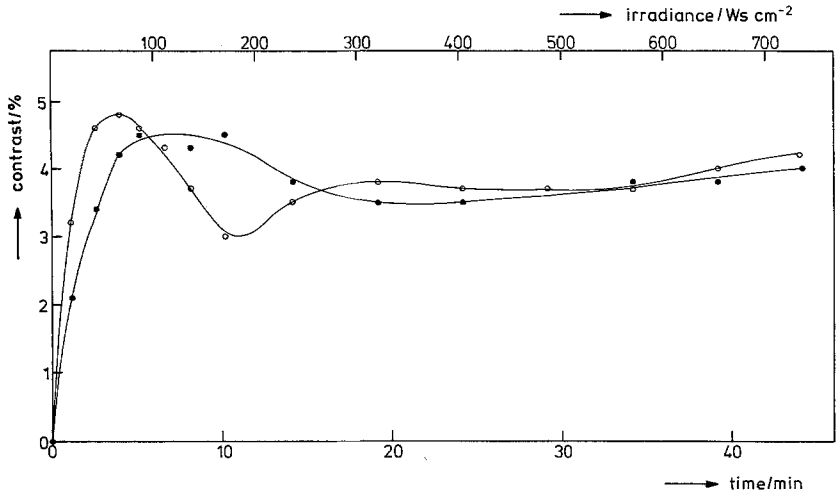

Fig. 4. Time development of the second Fourier component of the contrast, which appears in Fig. 3 at the space frequency 2.08 μm^{-1} (sample A). (a) during read out (full dots) with one incident beam at Bragg angle (b) during writing (open circles) with two interfering beams illuminating the grating. The lines connect the experimental points. The second harmonic rises faster in the writing pattern than in the readout pattern

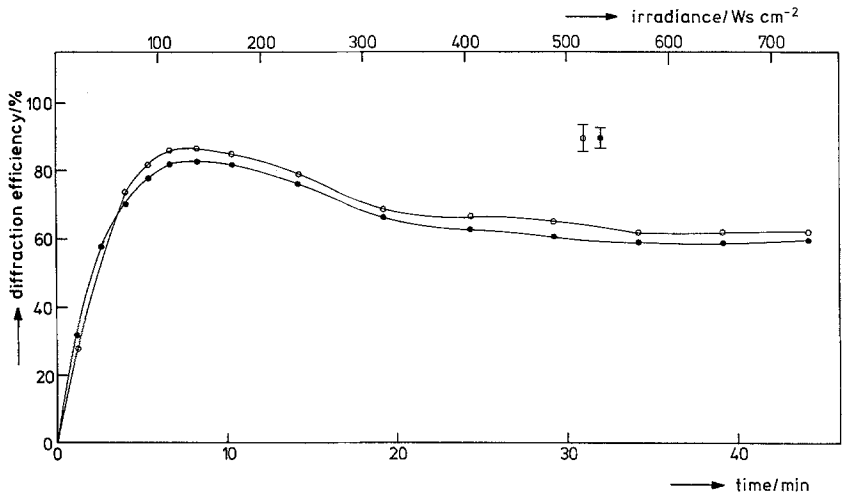

Fig. 5. Accordance of contrast and diffraction measurements obtained after correction of second-order contributions

Table 2. Measurement data of the holographic writing process

Measured					Calculated		
t	η_1	m_{012}	m_{02}	ϕ_{02}	m_{12}	m_{01}	η_1
[min]				[deg]			
1.3	0.318	0.88	0.021	179	0.015	0.90	0.28
2.7	0.572	0.98	0.034	221	0.039	1.0	0.50
4.0	0.709	0.85	0.042	240	0.068	0.88	0.74
5.3	0.782	0.74	0.045	248	0.092	0.77	0.82
6.7	0.818	0.66	0.043	248	0.102	0.69	0.86
8.2	0.832	0.63	0.043	244	0.108	0.66	0.87
10.2	0.823	0.67	0.045	236	0.104	0.72	0.85
14.2	0.758	0.77	0.038	222	0.071	0.82	0.79
19.2	0.666	0.88	0.035	202	0.051	0.92	0.69
24.2	0.628	0.90	0.035	188	0.047	0.94	0.67
29.2	0.605	0.91	0.037	171	0.047	0.95	0.65
34.3	0.594	0.93	0.038	162	0.046	0.97	0.62
39.2	0.591	0.93	0.038	154	0.046	0.97	0.62
44.2	0.597	0.93	0.040	157	0.049	0.97	0.62

3. Calculation of the Refractive Index Amplitude Considering Light-Induced Scattering

The measured refractive index amplitudes Δn, calculated with the help of (5), are represented in Fig. 6 as a function of the recording time (full dots). Usual arguments for the broad maximum, which can be seen, are easily ruled out:

1) Diffraction efficiency is far below 100%.

2) Since both writing beams have almost equal intensities no transient energy transfer occurs [13].

3) In a highly doped crystal, like the one under investigation, screening and transport lengths can be considered to be small.

Another reason, more likely than the three just mentioned, is light-induced scattering. It has been shown that the scattering process builds up essentially with the Maxwell relaxation time constant $\tau = \varepsilon\varepsilon_0/\sigma_{ph}$, which determines also the writing process [14]. Here ε is the static dielectric constant, ε_0 the vacuum permittivity and σ_{ph} the photoconductivity. Furthermore it is plausible, that the intensity I_s of the stray light gives rise to a bright background, which lowers the effective light intensity modulation

$$m(t) = \frac{2\sqrt{I_+(t)I_-(t)}}{I_+(t)+I_-(t)+I_s(t)}. \tag{6}$$

Since the intensity of the stray light is at each time equal to the intensity loss of the writing beams, we get for equal writing intensities $I_+(t) = I_-(t)$

$$m(t) = I_\pm(t)/I_\pm(0). \tag{7}$$

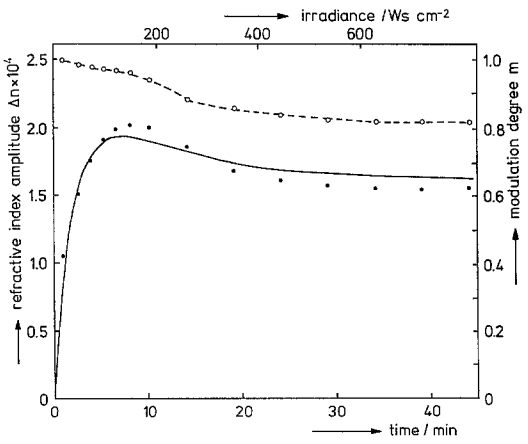

Fig. 6. Open circles represent the measurements of the modulation degree $m(t)$ defined by (6), which decays because of light-induced scattering. Full dots show the refractive index amplitude evaluated with the help of (5). After about 7 minutes a broad maximum appears. With the modulation degree curve (broken line, connecting the modulation degree data points) as input the time development of the refractive index amplitude was calculated (solid line) with the linear response model given by (8) and with $\Delta n_\infty = 1.65 \times 10^{-4}$ and $\tau = 1.7$ min

In fact a loss of 18% was finally observed as shown in Fig. 6 (open circles), which corresponds to a decay of the modulation down to 82%. Marotz et al. [15] describe the writing process by the linear response relation

$$\Delta n(t) = \int_{-\infty}^{+\infty} G(t-t')m(t')dt' \tag{8}$$

with

$$G(t) = (\Delta n_\infty/\tau m_\infty)\exp(-t/\tau)\Theta(t). \tag{9}$$

Here Δn_∞ is the saturation refractive index, m_∞ the saturation modulation and $\Theta(t)$ the Heaviside step function.

The solid line shown in Fig. 6 results from (8) with the experimental parameters $\tau = 1.7$ min, $\Delta n_\infty = 1.65 \times 10^{-4}$ and the time dependent modulation represented by the measured data shown in Fig. 6 (open circles). The success shows that light induced scattering can indeed be taken into account using (8).

4. Experimental Results for the Light Intensity Pattern During Writing

The interference pattern of the two beams writing the grating can be observed at the exit face of the sample. We call this pattern the "writing pattern" to distinguish it from the interference pattern, which is generated during readout at Bragg angle by one beam alone and which we call furtheron the "readout pattern". While the readout pattern yields information on the grating (amplitude and phase shift), the writing pattern reflects the dynamic feedback process between grating and electromagnetic field, which has its deeper origin in the fact, that the photorefractive writing process is nonlocal. In later statements on grating phase shifts derived from the readout pattern, we allow for the phase difference of $\pi/2$ between this pattern and the grating.

Since a just written grating is phase shifted with respect to the writing pattern (Fig. 7a), the writing pattern will change in turn (Fig. 7b). Thus we observe, in fact, both patterns shifting with time in a dynamic feedback process until the shifts finally become stationary. The phase shift ϕ_g of the refractive index grating reaches its maximum earlier than the shift Φ of the readout pattern. If we compare the phase shift of the readout pattern with the diffraction efficiency, they seem to change simultaneously. As a result, the time dependent phase difference $\phi = \Phi - \phi_g$ becomes maximal at a somewhat later time (Fig. 8a).

A surprising consequence of the photorefractive writing feedback process is the development of a second Fourier component in the contrast spectrum of

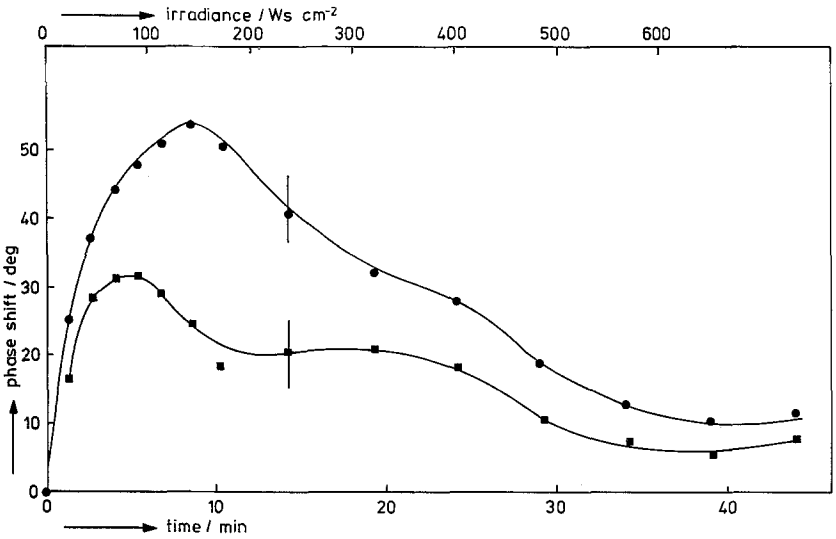

Fig. 7. Direct phase shift measurements at several stages of the writing process (sample A). Reference pattern is the writing pattern at the time $t=0$ with the attributed phase $\Phi=0$. (a) Phase ϕ_g of the refractive index grating (full squares) evaluated from the reading pattern. (b) Phase Φ of the writing pattern (full dots) at the exit face of the crystal

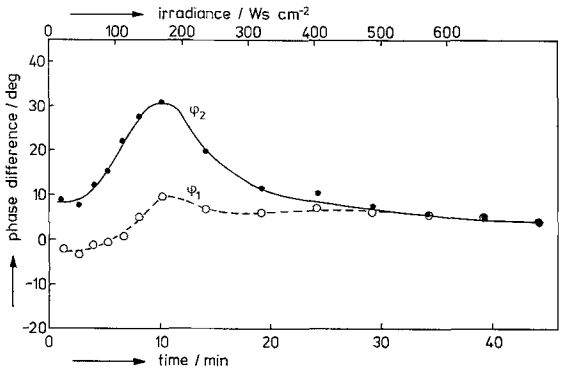

Fig. 8. Phase difference between grating and writing pattern at the exit face of the sample A. (a) direct measurements by microphotometry (full dots) (b) computed from transient energy transfer (open circles) via 10 and 11

the writing pattern which is plotted in Fig. 4 (open circles). We would like to draw special attention to the fact, that this component grows faster than the corresponding component in the readout pattern. This fact is underlined in Fig. 9 by the results of sample B, which has been recorded with lower writing intensity, thus leading to a better time resolution. The contrast of both patterns approaches nearly the same saturation values. For these findings we propose the following explanation:

The interference field in a modulated medium is no longer described by the interference of two plane waves but by the interference of two Bloch waves. Consequently the Fourier decomposition always contains higher-order contributions, the second-order being the next largest after the fundamental first order. Subsequently this Fourier component of second order in the writing pattern makes a contribution to the development of a second-order Fourier component Δn_2 of the refractive index amplitude, which in turn may intensify the second-order Fourier component of the Bloch wave (the wave equation is now no longer a Mathieu equation, but adequately described by Hill's equation). The nonlinear quality of the read-write feedback process causes in this way a nonlinear recording, even if the photorefractive recording process is strictly linear and exactly described by (8). In fact, it is not and this possibly favours the mentioned feedback. To our knowledge this source of nonlinearity on principle has never been realized.

The results on the phase difference ϕ between writing pattern and grating will now be discussed in regard of the energy transfer between the writing beams and its consequences for the first-order Fourier component of the writing pattern. Starting from equal intensities at the entrance face of the grating, i.e. $I_{+10}=I_{-10}=I_0$, the intensity of one beam, say I_{+1}, is enhanced on the cost of the intensity I_{-1} of the other beam by an amount depending on the phase difference ϕ and the grating amplitude. This effect, first mentioned by Staebler and Amodei [16], follows the equations

$$I_{+1}=I_0[1+\sin(2\delta)\sin\phi], \tag{10}$$

$$I_{-1}=I_0[1-\sin(2\delta)\sin\phi], \tag{11}$$

where $\delta=\pi\Delta n/\lambda_0\cos\Theta$. Results on the phase shift ϕ evaluated from the measured energy transfer during writing via (10 and 11) are represented in Fig. 8b by open circles. Yet we do not know, why these results differ from the direct microscopic determination of the phase shifts, also shown in Fig. 8a.

Because the energy transfer changes the intensity ratio between writing beams, the light intensity modulation of the writing interference pattern will be affected by this. Fortunately the contrast of the writing pattern

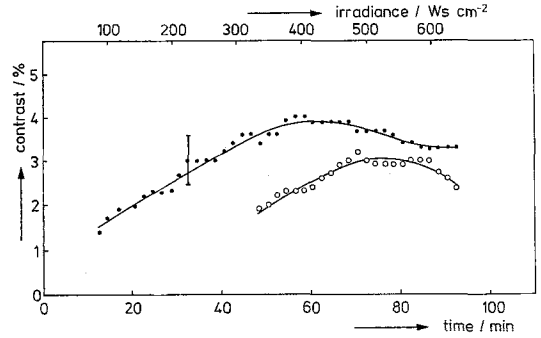

Fig. 9. The second contrast Fourier component rises much faster in the writing pattern (full circles) than in the readout pattern (open circles). Lines connect the measurement points. Data with contrast lower than 1% were omitted, because of spreading noise contributions (sample B)

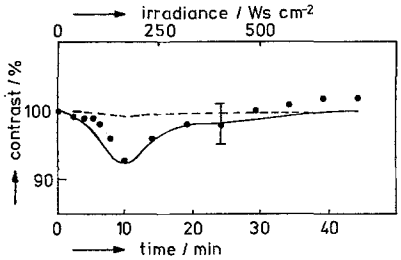

Fig. 10. First contrast Fourier component of the writing pattern of sample A. Full line: calculated from direct phase difference measurements. Dashed line: from intensity transfer between writing beams via (12). The contrast of the first pattern was set to 100%. Note that the contrast, defined here as the first Fourier component of the intensity pattern, may exceed 100% due to higher diffraction orders

measured by the imagine system is hardly influenced by the light-induced scattering discussed in Sect. 3. This happens, because most of the intensity is scattered outside of the limiting objective aperture of the microscope. Inserting (10 and 11) into (6) and neglecting the scattering contribution to the total intensity because of the reason just mentioned yields

$$m(t)=\sqrt{1-\sin^2(2\delta d)\sin^2(\phi)}\,. \tag{12}$$

Experimental points obtained from the first-order Fourier component of the writing pattern at the exit face of the sample are shown in Fig. 10 together with curves based on direct observation of the phase difference (full line) and on phase difference values derived from energy transfer measurements (dashed line). The curves are calculated with (12). The measurement points confirm a decay of the modulation degree in virtue of a phase difference. The time at which the modulation passes a minimum corresponds to the time for maximum phase difference. It should be mentioned that the first-order Fourier component of the writing pattern exceeds 100% at the end of the recording process. This indicates once more that Fourier components of higher order are present and a two-beam description is not satisfactory.

The just discussed decrease of the modulation degree is of importance for the theory of holographic writing in photorefractive crystals. It is very helpful to look at the phenomenon from a different point of view and to consider it as a Moiré-like effect. Then we should expect – in accordance with (12) – to observe a variation of the contrast at the exit face of the grating (i.e., a contrast becoming periodically stronger and weaker) as we translate the grating relative to the interference pattern in a direction parallel to the grating vector. This is just what we find by performing such experiments with a piezo-driven translation table. Hence the beam-coupling is in a sense the repercussion of the Moiré-effect on the far-field intensity pattern.

These results clearly demonstrate, that the method of direct imaging of refractive-index gratings offers new possibilities for the study of the photorefraction process.

5. Conclusions

The microphotometric method introduced previously [6] has been applied to the investigation of the recording process in photorefractive crystals. A comparison of diffraction efficiency measurements with the first-order Fourier coefficient of the intensity pattern shows the high sensitivity of the method to higher diffraction orders. The two-beam approximation is not sufficient for a description of the experimental results. Some advantages of the microphotometric investigation method have been demonstrated, namely the possibility to determine the contrast and the phase shift of the light intensity pattern at the exit face of the sample as well as of the refractive index grating independently, including also higher-order Fourier components in the investigations. A fundamental source of nonlinearity in the writing process of gratings has been pointed out and evidence to a Moiré-like effect has been given, which causes the modulation degree to change during writing due to the relative phase shift between light intensity pattern and grating. The refractive index amplitude has been calculated in the presence of light induced scattering.

Acknowledgements. I thank E. Krätzig for his continuous support and discussions. Valuable discussions with my colleagues, especially with H. Vormann and K. Ringhofer are greatfully acknowledged. This work has been performed within the program of the "Sonderforschungsbereich 225 'Oxide Crystals for Electro- and Magnetooptic Applications" supported by the "Deutsche Forschungsgemeinschaft".

References

1. P. Günter: Phys. Rep. **93**, 199 (1982)
2. R.J. Woods, L. Young: Ferroelect. **46**, 275 (1983)
3. K.H. Richter, W. Güttler, M. Schwoerer: Appl. Phys. A **32**, 1 (1983)
4. R. Baltz, C. Lingenfelder, R.A. Rupp: Appl. Phys. A **32**, 13 (1983)
5. R.A. Rupp, E. Krätzig: Phys. Stat. Solidi (a) **72**, K5 (1982)
6. R.A. Rupp: Appl. Phys. B **41**, 153–168 (1986)
7. P.St. J. Russel: Opt. Commun. **46**, 71 (1983)
8. T. Tamir, H.C. Wang, A.A. Oliner: IEEE Trans. MTT-**12**, 323 (1964)
9. T. Tamir: Math. Comput. **16**, 100 (1962)
10. C. Burckhardt: J. Opt. Soc. Am. **56**, 1502 (1966)
11. R.A. Rupp, G. Wittenbecher, E. Krätzig: To be published
12. E. Guibelalde: Opt. Quant. Electron. **16**, 173 (1984)
13. N. Kukhtarev, V. Markov, S. Odulov: Opt. Commun. **23**, 338 (1977)
14. R.A. Rupp, F.W. Drees: Appl. Phys. B **39**, 223 (1986)
15. J. Marotz, K. Ringhofer, R.A. Rupp, S. Treichel: IEEE J. QE-**22**, 1376 (1986)
16. D.L. Staebler, J.J. Amodei: J. Appl. Phys. **43**, 1042 (1972)